Electronic Supplementary Material (ESI) for Physical Chemistry Chemical Physics.

Electronic Supplementary Information for

Magnetic semiconducting borophenes and their derivatives

Bo Chen,* Lin Xue, Yan Han, Zhi Yang and Yong-Jia Zhang
College of Physics, Taiyuan University of Technology, Taiyuan 030024, P. R. China
Corresponding author Email: chenbo@tyut.edu.cn

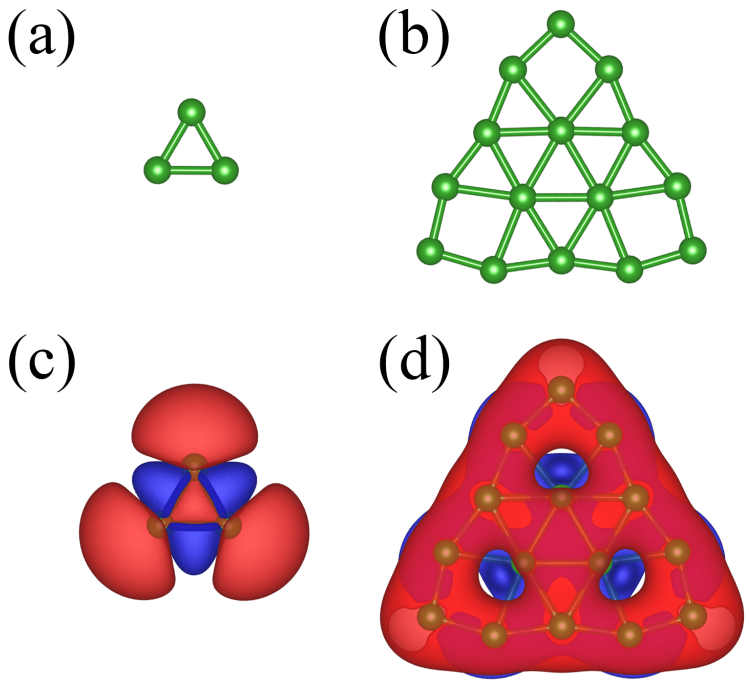

Figure S1. (a-b) Optimized structures and (c-d) corresponding spin charge density distributions of B_3 and B_{15} triangular motifs. The red/blue color denotes electron spin up/down, respectively.

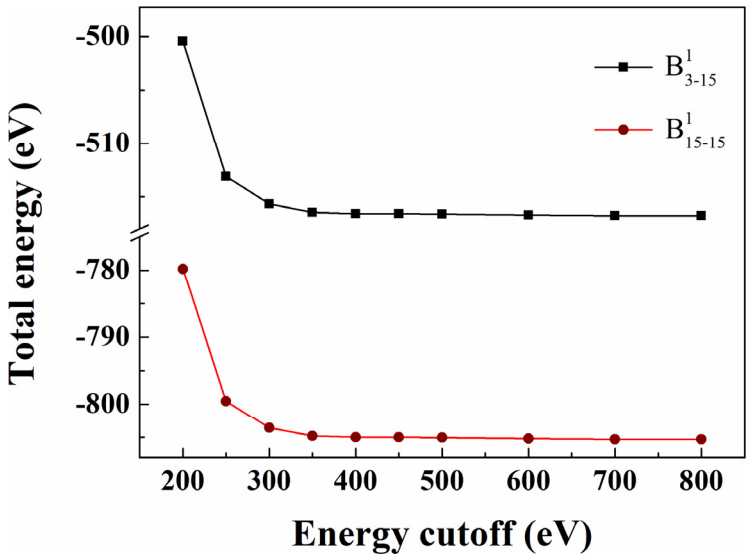

Figure S2. Total energies of 2×2 supercells for FM $B^1_{3\text{-}15}$ and $B^1_{15\text{-}15}$ monolayers versus the energy cutoff.

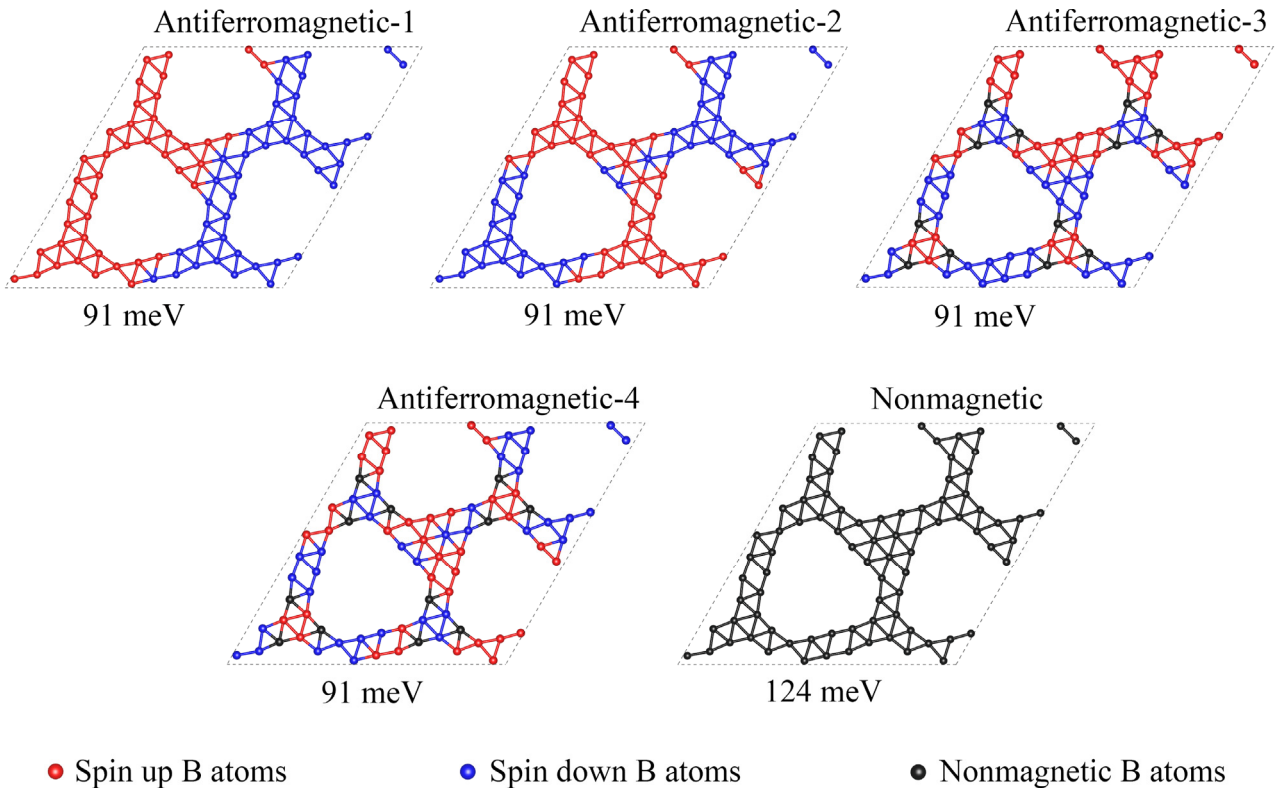

Figure S3. Geometric structures for 2×2 supercells of monolayer $B^{1}_{3\text{-}15}$ in AFM and NM configurations, and their corresponding relative energies with respect to the FM state shown in the left panel of Fig. 1 in the main text.

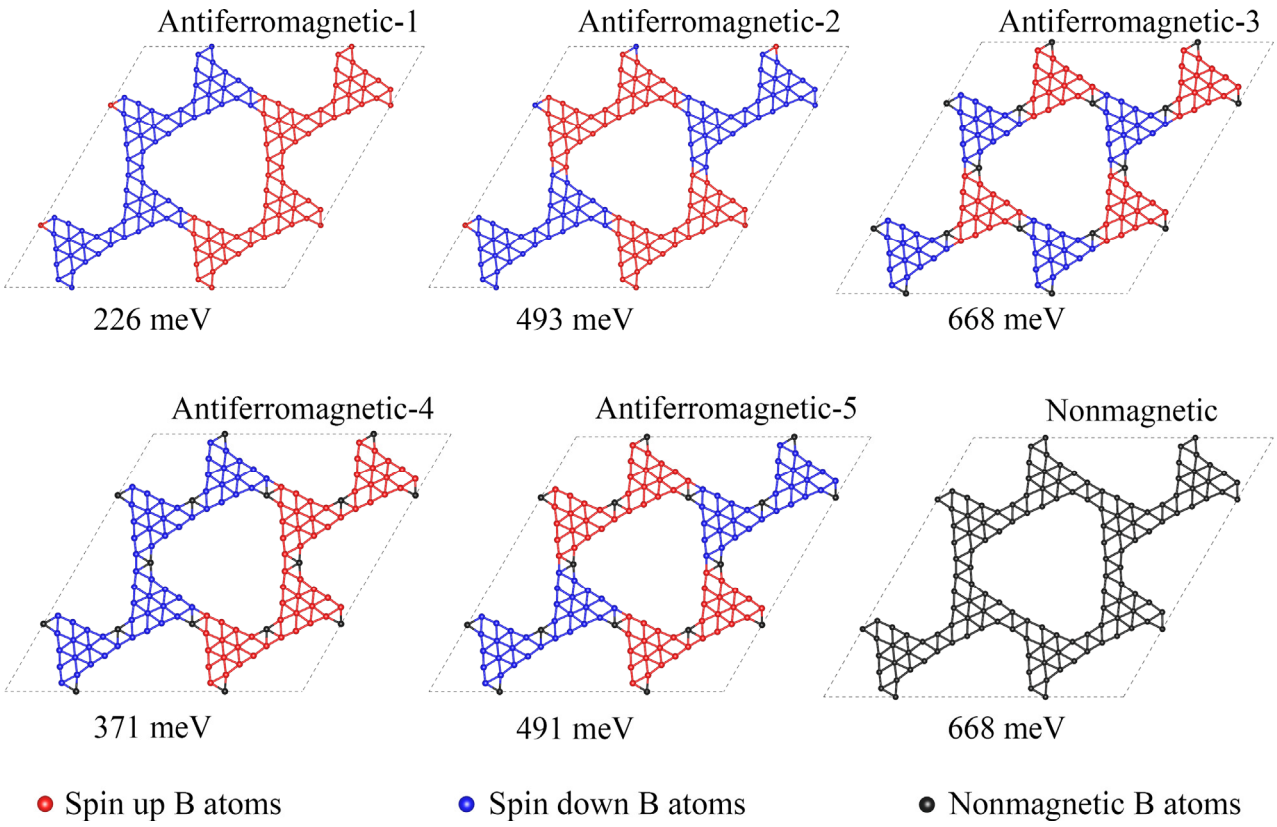

Figure S4. Geometric structures for 2×2 supercells of monolayer $B^{1}_{15\text{-}15}$ in AFM and NM configurations, and their corresponding relative energies with respect to the FM state shown in the right panel of Fig. 1 in the main text.

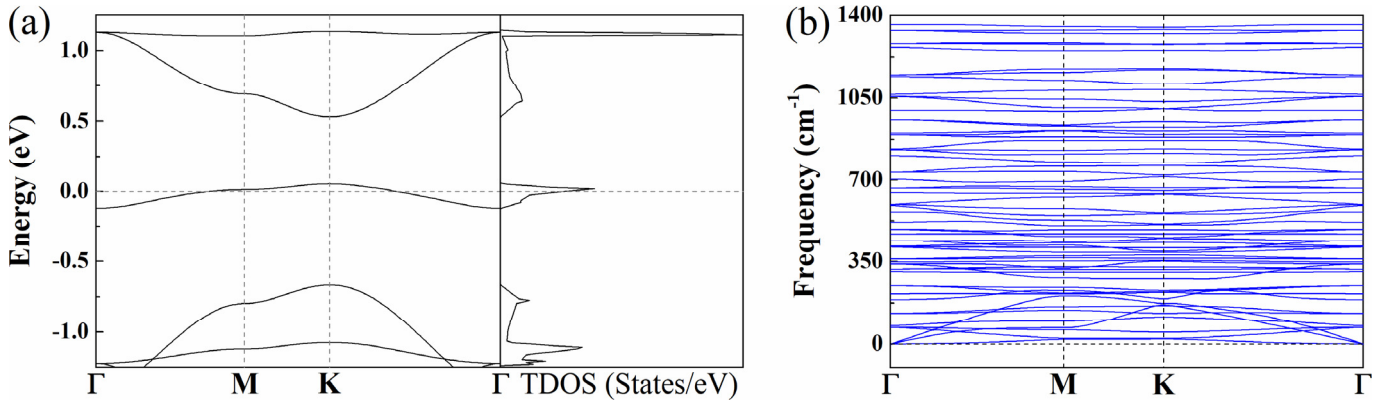

Figure S5. (a) Band structure, total density of states (TDOS), and (b) phonon spectrum for monolayer $B^{1}_{3\text{-}15}$ with NM ordering. The Fermi level in (a) is set to zero.

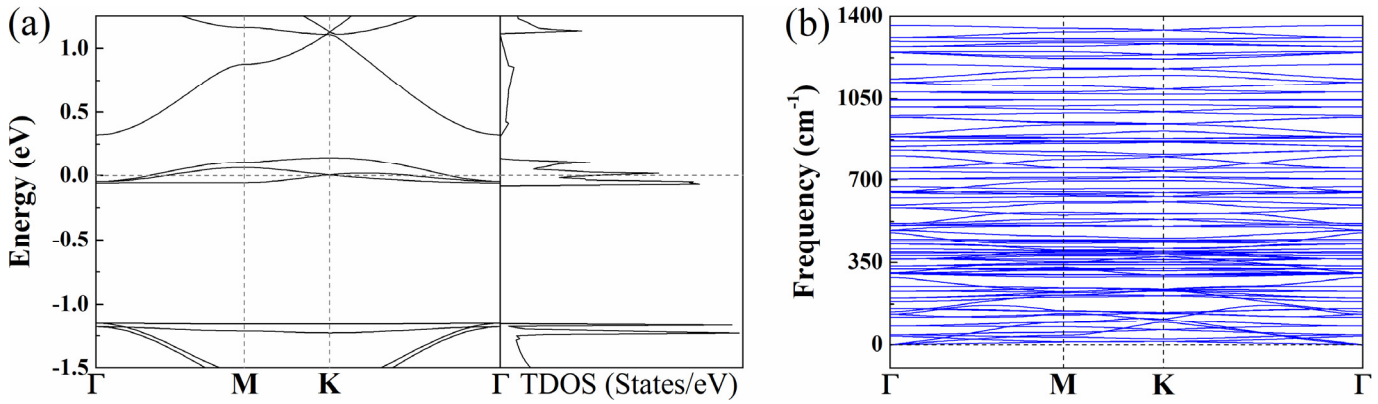

Figure S6. (a) Band structure, TDOS, and (b) phonon spectrum for monolayer $B^{1}_{15\text{-}15}$ with NM ordering. The Fermi level in (a) is set to zero.

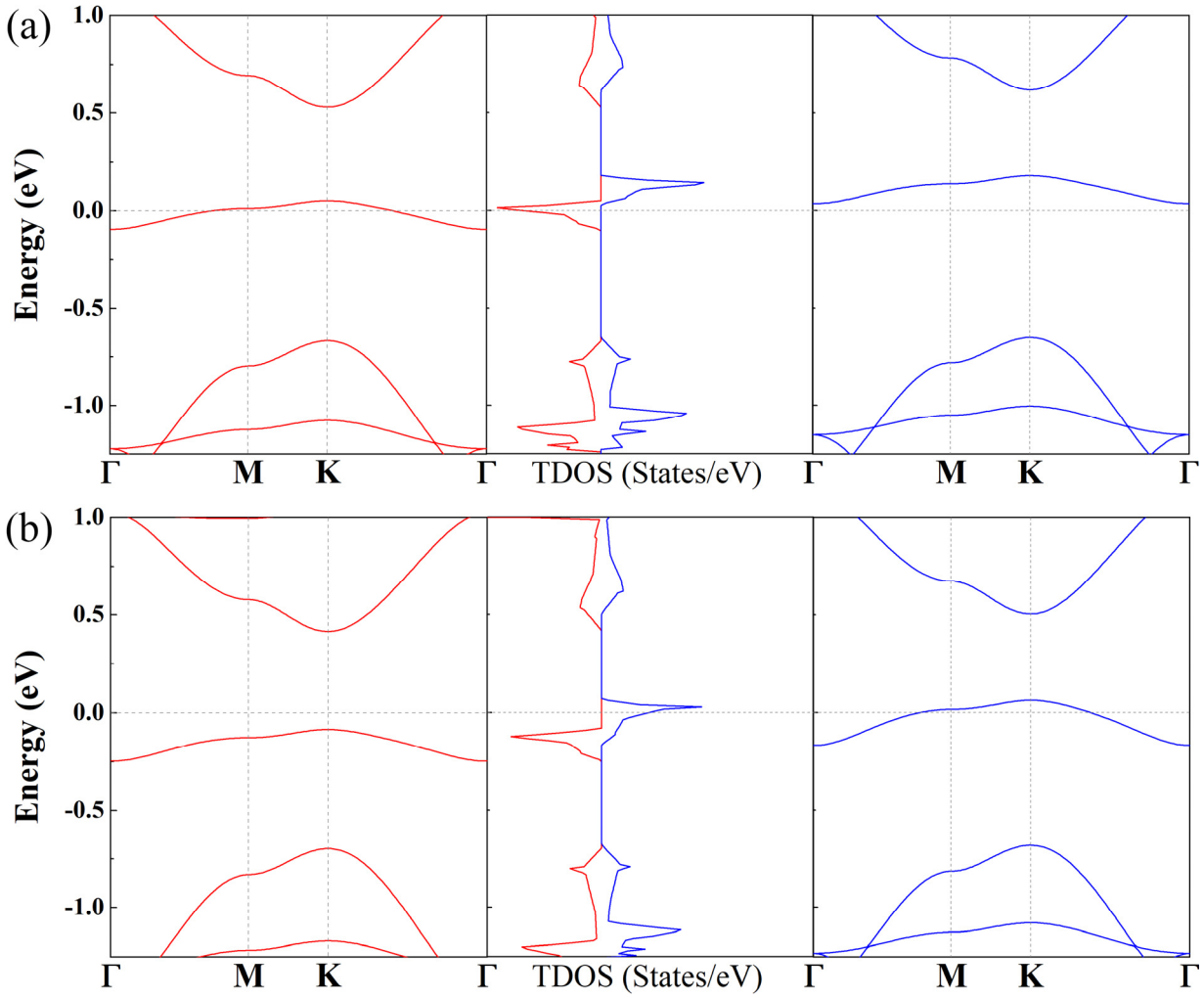

Figure S7. Band structures and TDOS of (a) hole doped and (b) electron doped FM $B^{1}_{3\text{-}15}$ monolayer, calculated at the PBE level of theory. The doping concentration is -0.5*e*/0.5*e* per primitive cell for hole/electron doping. Fermi energy is set to zero.

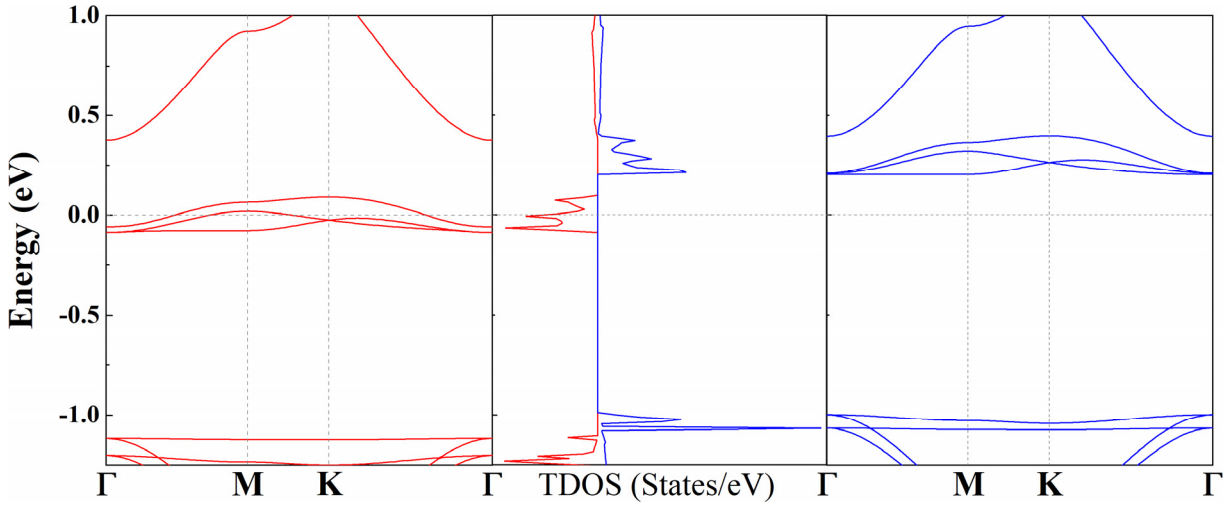

Figure S8. Band structures and TDOS of hole doped FM $B^{1}_{15\text{-}15}$ monolayer, calculated at the PBE level of theory. The doping concentration is -*e* per primitive cell. Fermi energy is set to zero.

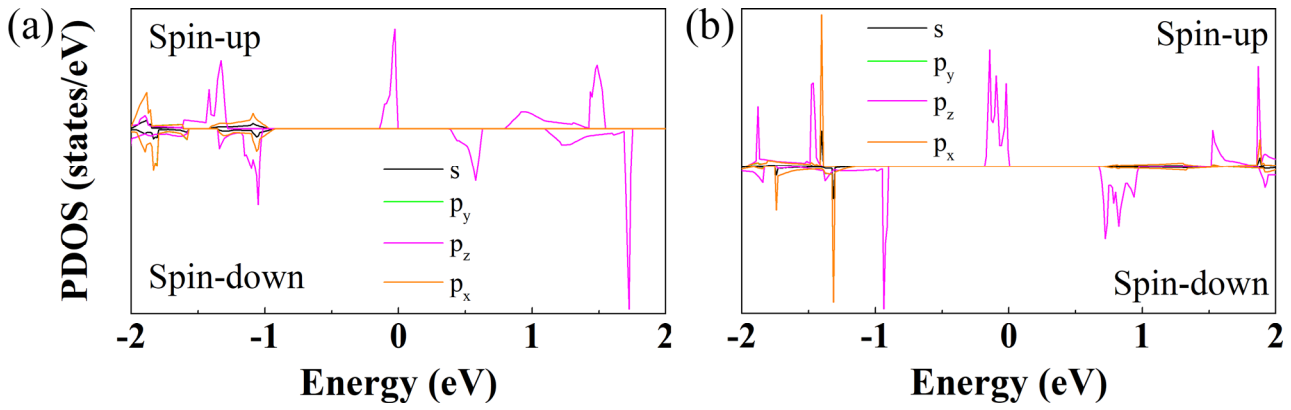

Figure S9. Projected density of states (PDOS) for monolayer (a) $B^{1}_{3\text{-}15}$ and (b) $B^{1}_{15\text{-}15}$ at FM ground state. Fermi level is set as zero.

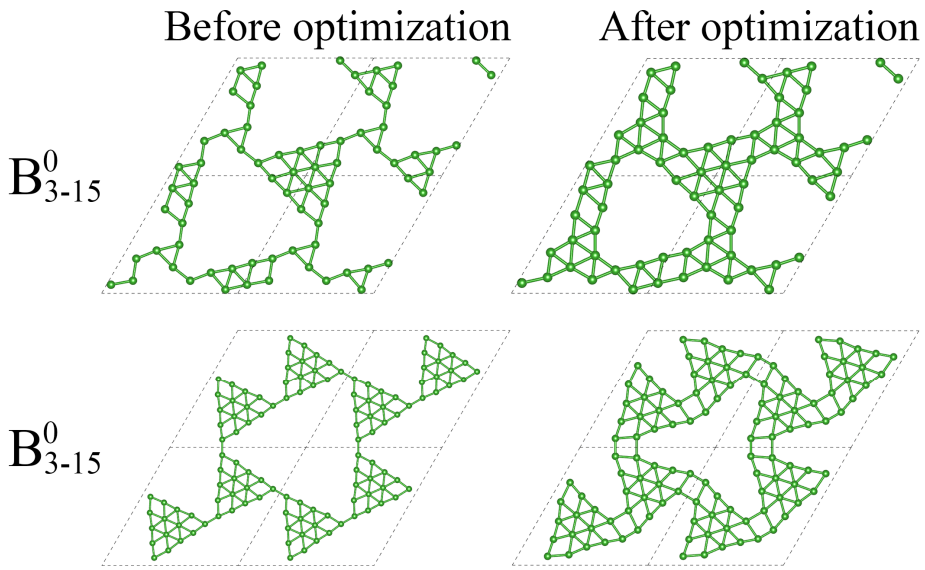

Figure S10. Top view of the initial and optimized structures for monolayer $B^{0}_{3\text{-}15}$ and $B^{0}_{15\text{-}15}$.

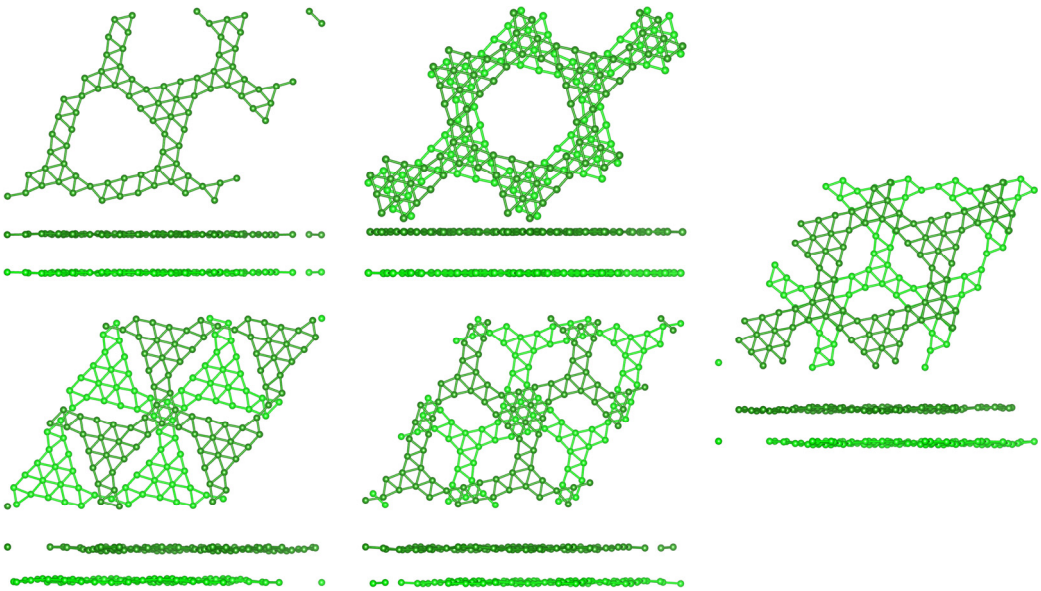

Figure S11. Schematics of the high-symmetry stackings in bilayer $B^{1}_{3\text{-}15}$. Different boron atomic layers are distinguished by color.

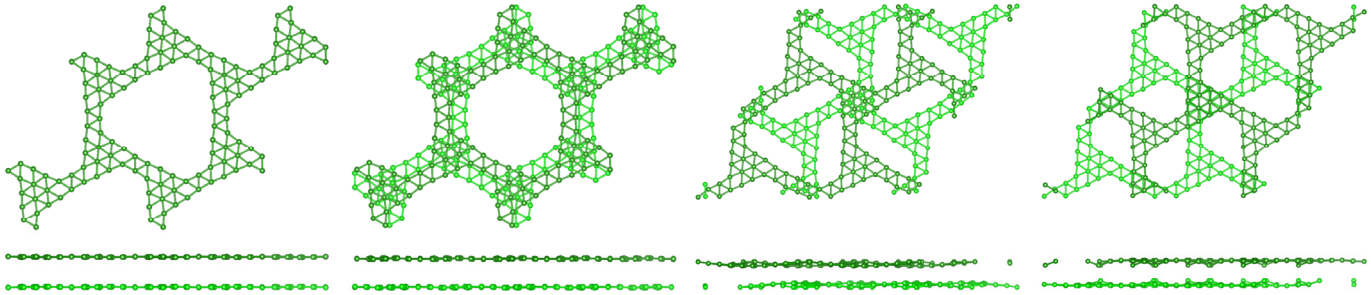

Figure S12. Schematics of the high-symmetry stackings in bilayer $B^{1}_{15\text{-}15}$. Different boron atomic layers are distinguished by color.

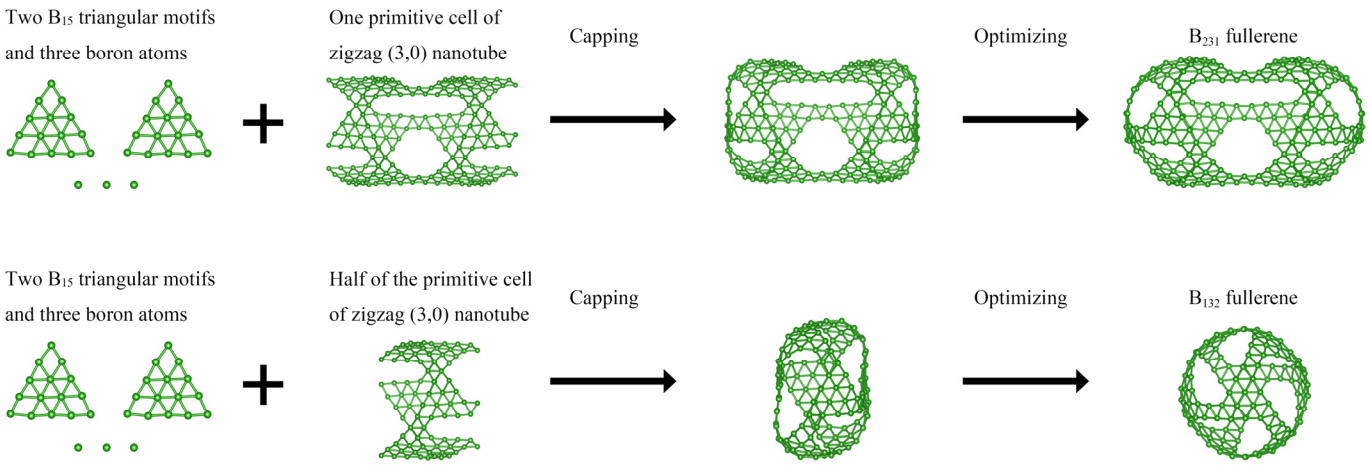

Figure S13. Manufacture processes of the B_{231} (up panel) and B_{132} (lower panel) fullerenes.

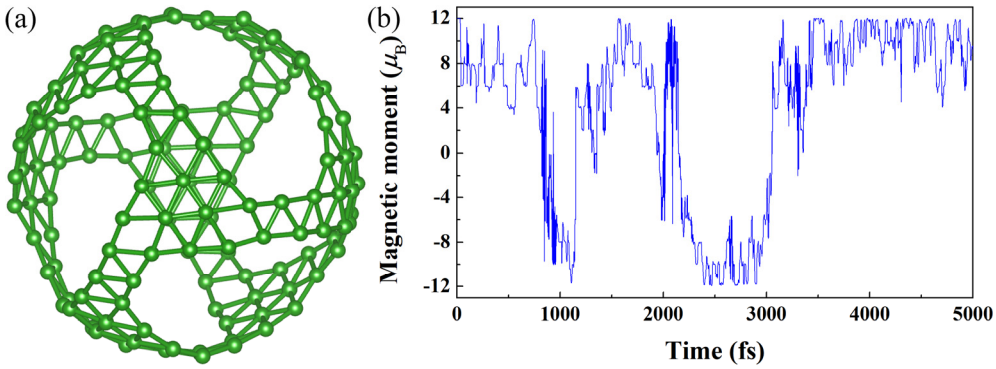

Figure S14. (a) Snap shot of B_{132} fullerene at the end of *ab initio* molecular dynamics simulation performed at 300 K for 5 ps, and (b) the corresponding change of total magnetic moment with simulation time step.

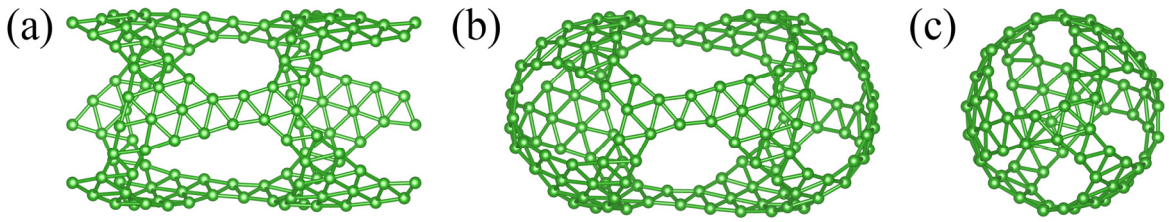

Figure S15. Optimized structures of (a) zigzag (3,0) nanotube with magnetic moment of about 6.00 μ_B per primitive cell, (b) B_{147} and B_{84} fullerenes with total magnetic moment of 6.48 and 2.00 μ_B, respectively. Nanotube and fullerenes are built based on the monolayer $B^1_{3\text{-}15}$ borophene.

Similarly, magnetic B_{63m+21} fullerenes could be constructed via capping the zigzag (3,0) nanotube with one B_{15} triangular motif, one B_3 triangular motif, and three boron atoms, where m is a positive integer and the number of half of the primitive cell of zigzag (3,0) nanotube built based on the monolayer $B^1_{3\text{-}15}$ borophene.

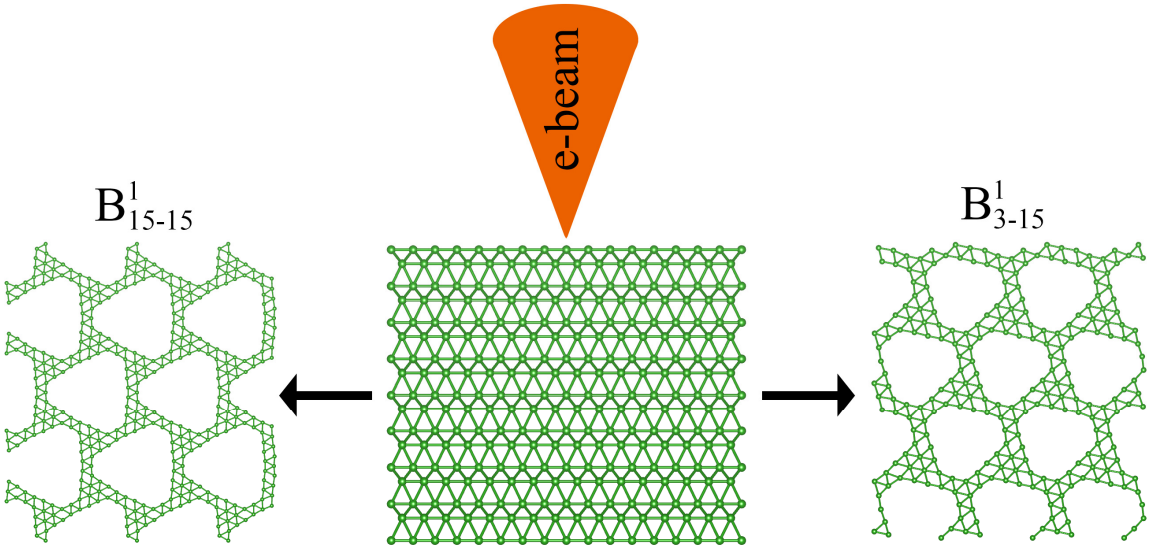

Figure S16. Schematic illustration of the e-beam fabrication of monolayer $B^1_{3\text{-}15}$ and $B^1_{15\text{-}15}$ borophenes by selective sputtering the boron atoms from a freestanding borophene in buckled triangular structure.